Numerical Solutions of Peristaltic Flow of a Jeffrey-Six Constant Fluid with Variable Magnetohydrodynamic

Sohail Nadeem and Noreen Sher Akbar

Department of Mathematics, Quaid-i-Azam University 45320, Islamabad 44000, Pakistan

Reprint requests to S. N.; E-mail: snqau@hotmail.com

Z. Naturforsch. **65a,** 911 – 918 (2010); received August 13, 2009 / revised December 10, 2009

In the present article we have studied the magnetohydrodynamic (MHD) peristaltic flow of a Jeffrey-six constant fluid in an endoscope. We have simplified the governing equations of such a fluid under the assumptions of long wave length and low Reynolds number approximation. The reduced momentum equations are solved by (i) the homotopy analysis method (HAM) and (ii) the shooting method. The comparison of both solutions is presented. Velocity profile, streamlines, and convergence region are discussed graphically for different values of Hartmann number M, and Jeffrey parameter λ_1 and λ_2.

Key words: Peristaltic Flow; Jeffrey-Six Constant Fluid; Endoscope; HAM Solution; Numerical Solution; Variable MHD.

1. Introduction

The peristaltic flow is a form of fluid transport which occurs in many biological systems such as urine transport from kidney to bladder through the ureter, movement of chyme in the gastrointestinal tract, movement of spermatozoa in the ducts afferents of the male reproductive tract and the ovum in the female fallopian tube, locomotion of some worms, transport of lymph in the lymphatic vessels, and vasomotion of small blood vessels such as arterioles, venules, and capillaries. This mechanisms of fluid transport has received considerable attention in recent times in engineering as well as in physiological sciences due to its wide range of applications in industry and physiology. Some recent investigations which studies the peristaltic phenomena according to different flow geometries are studied in [1 – 8]. The magnetohydrodynamic (MHD) flow of a fluid in a tube or channel with peristalsis is of interest in connection with certain problems of the movement of conductive physiological fluids, e. g., the blood in blood pump machines and with the need for theoretical research on the operation of a peristaltic MHD compressor. Hydromagnetic flow of fluid with variable viscosity in a uniform tube with peristalsis was studied by Hakeem et al. [9], and they analyzed that the magnetic field accelerates the speed of blood. T. Srinivas et al. [10] considered the influence of slip conditions, wall properties and heat transfer on MHD third-grade fluid in a deformable tube. Some other papers dealing with MHD flows of peristaltic are [11 – 15]. Recently, Srinivas and Kothandapani [16] have discussed the mixed convection with heating effects in a vertical porous annulus with radially varying magnetic field. Such a field is important in engineering.

To see the importance of radially varing MHD we have studied the peristaltic flow of a Jeffrey-six constant fluid model [17] with variable MHD in an endoscope. The governing equations have been simplified using the assumption of long wave length and low Reynolds number approximation. Analytical and numerical solutions have been derived for both constant and variable MHD cases. The physical behaviour of the velocity profile has been discussed for various parameters of interest.

2. Mathematical Formulation

Let us consider the peristaltic transport of an incompressible six-constant Jeffreys fluid in two concentric tubes. The flow is generated by sinusoidal wave trains propagating with constant speed c_1 along the walls of the tubes. The geometry of the wall surface is defined as

$$\bar{R}_1 = a_1, \tag{1}$$

$$\bar{R}_2 = a_2 + b_1 \sin \frac{2\pi}{\lambda}(\bar{Z} - c_1 \bar{t}), \tag{2}$$

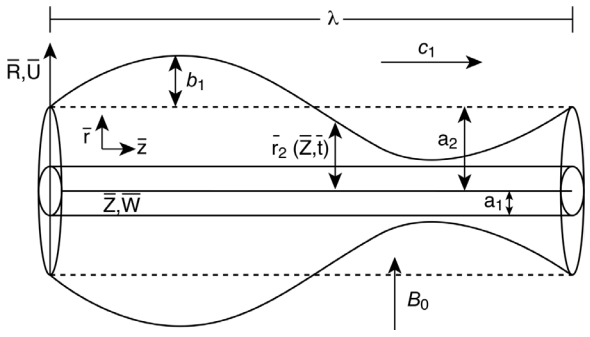

Fig. 1. Geometry of the problem.

where a_1 and a_2 are the radius of the inner and outer tubes at inlet, b_1 is the wave amplitude, λ is the wavelength, c is the propagation velocity, and $\bar{t}$ is the time. We are considering the cylindrical coordinate system $(\bar{R},\bar{Z})$, such that the $\bar{Z}$-axis lies along the center line of the tubes, and $\bar{R}$ is transverse to it.

The governing equations in the fixed frame for an incompressible flow are

$$\frac{\partial \bar{U}}{\partial \bar{R}}+\frac{\bar{U}}{\bar{R}}+\frac{\partial \bar{W}}{\partial \bar{Z}}=0, \tag{3}$$

$$\rho\left(\frac{\partial}{\partial \bar{t}}+\bar{U}\frac{\partial}{\partial \bar{R}}+\bar{W}\frac{\partial}{\partial \bar{Z}}\right)\bar{U}= -\frac{\partial \bar{P}}{\partial \bar{R}}+\frac{1}{\bar{R}}\frac{\partial}{\partial \bar{R}}(\bar{R}\bar{T}_{\bar{R}\bar{R}})+\frac{\partial}{\partial \bar{Z}}(\bar{T}_{\bar{R}\bar{Z}})-\frac{\bar{T}_{\bar{\theta}\bar{\theta}}}{\bar{R}}, \tag{4}$$

$$\rho\left(\frac{\partial}{\partial \bar{t}}+\bar{U}\frac{\partial}{\partial \bar{R}}+\bar{W}\frac{\partial}{\partial \bar{Z}}\right)\bar{W}= -\frac{\partial \bar{P}}{\partial \bar{Z}}+\frac{1}{\bar{R}}\frac{\partial}{\partial \bar{R}}(\bar{R}\bar{T}_{\bar{R}\bar{Z}})+\frac{\partial}{\partial \bar{Z}}(\bar{T}_{\bar{Z}\bar{Z}})-\sigma(B_0(r))^2\bar{W}. \tag{5}$$

The extra stress tensor for a six-constant Jeffreys fluid model is given by [17]

$$\bar{T}+\varepsilon_1\left[\frac{\mathrm{d}\bar{T}}{\mathrm{d}t}-W\cdot\bar{T}+\bar{T}\cdot W+d(\bar{T}\cdot D+D\cdot\bar{T})+b\bar{T}:D\mathbf{I}+cD\mathrm{tr}\bar{T}\right]= 2\mu\left[D+\varepsilon_2\left(\frac{\mathrm{d}D}{\mathrm{d}t}-W\cdot D+D\cdot W+2dD\cdot D+bD:DI\right)\right], \tag{6}$$

where

$$D=\frac{\nabla\bar{\mathbf{V}}+(\nabla\bar{\mathbf{V}})^{\mathbf{T}}}{2},\quad W=\frac{\nabla\bar{\mathbf{V}}-(\nabla\bar{\mathbf{V}})^{\mathbf{T}}}{2}. \tag{7}$$

D is the symmetric part of the velocity gradient, W the antisymmetric part of the velocity gradient, d, b, c are material constant of the six-constant Jeffreys fluid model, ε_1 is the relaxation time, and ε_2 is the delay time.

Introducing a wave frame $(\bar{r},\bar{z})$ moving with velocity c_1 away from the fixed frame $(\bar{R},\bar{Z})$ by the transformations

$$\bar{z}=\bar{Z}-c_1\bar{t},\quad \bar{r}=\bar{R}, \tag{8}$$

$$\bar{w}=\bar{W}-c_1,\quad \bar{u}=\bar{U}, \tag{9}$$

where $\bar{U}$, $\bar{W}$ and $\bar{u}$, $\bar{w}$ are the velocity components in the radial and axial directions in the fixed and moving coordinates, respectively.

The corresponding boundary conditions are the no-slip at both walls

$$\begin{aligned}&\bar{u}=0,\ \bar{w}=-c_1\quad \text{at } \bar{r}=\bar{r}_1,\\ &\bar{u}=-c_1\frac{\mathrm{d}\bar{r}_2}{\mathrm{d}z},\quad \bar{w}=-c_1\\ &\text{at }\ \bar{r}=\bar{r}_2=a+b_1\sin\frac{2\pi}{\lambda}(\bar{z}).\end{aligned} \tag{10}$$

Further, we define

$$\begin{aligned}&R=\frac{\bar{R}}{a_2},\quad r=\frac{\bar{r}}{a_2},\quad Z=\frac{\bar{Z}}{\lambda},\quad z=\frac{\bar{z}}{\lambda},\\ &W=\frac{\bar{W}}{c_1},\quad w=\frac{\bar{w}}{c_1},\quad T=\frac{a_2\bar{T}}{c_1\mu},\quad U=\frac{\lambda\bar{U}}{a_2c_1},\\ &u=\frac{\lambda\bar{u}}{a_2c_1},\quad P=\frac{a_2^2\bar{P}}{c_1\lambda\mu},\quad t=\frac{c_1\bar{t}}{\lambda},\\ &\delta=\frac{a_2}{\lambda},\quad \mathrm{Re}=\frac{\rho c_1a_2}{\mu},\quad r_2=\frac{\bar{r}_2}{a_2},\\ &\lambda_1=\frac{\varepsilon_1c_1}{a_2},\quad \lambda_2=\frac{\varepsilon_2c_1}{a_2},\quad \varepsilon=\frac{b_1}{a_2}\ll 1,\\ &M=\sqrt{\frac{\sigma}{\mu}}B_0a_2.\end{aligned} \tag{11}$$

Using the above non-dimensional quantities and the transformation given in (8) and (9), the resulting equations can be written as

$$\frac{\partial u}{\partial r}+\frac{u}{r}+\frac{\partial w}{\partial z}=0, \tag{12}$$

$$\mathrm{Re}\,\delta^3\left(u\frac{\partial}{\partial r}+w\frac{\partial}{\partial z}\right)u= -\frac{\partial P}{\partial r}+\frac{\delta}{r}\frac{\partial}{\partial r}(rT_{rr})+\delta^2\frac{\partial}{\partial z}(T_{rz})-\frac{\delta T_{\theta\theta}}{r}, \tag{13}$$

$$\operatorname{Re}\delta\left(u\frac{\partial}{\partial r}+w\frac{\partial}{\partial z}\right)w = -\frac{\partial P}{\partial z}+\frac{1}{r}\frac{\partial}{\partial r}(rT_{rz})+\delta\frac{\partial}{\partial z}(T_{zz})-(M(r))^2(w+1), \tag{14}$$

where

$$T_{rz}=\frac{\partial w}{\partial r}\left[1+\lambda_1\lambda_2\left(1-d(d+b)-\frac{c}{2}(2d+3b)\right)\left(\frac{\partial w}{\partial r}\right)^2\right]\cdot\left[1+\lambda_1^2\left(1-d(d+b)-\frac{c}{2}(2d+3b)\right)\left(\frac{\partial w}{\partial r}\right)^2\right]^{-1},$$

$$T_{rr}=\lambda_2\left(\frac{\partial w}{\partial r}\right)^2(1+d+b)-\lambda_1\left(\frac{\partial w}{\partial r}\right)(1+d+b)T_{rz},$$

$$T_{zz}=\lambda_2\left(\frac{\partial w}{\partial r}\right)^2(-1+d+b)-\lambda_1\left(\frac{\partial w}{\partial r}\right)(-1+d+b)T_{rz},$$

$$T_{\theta\theta}=\lambda_2\left(\frac{\partial w}{\partial r}\right)^2 b-\lambda_1\left(\frac{\partial w}{\partial r}\right)bT_{rz},$$

where δ and Re represent the wave and the Reynolds number, respectively.

Under the assumption of long wave length approximation and low Reynold number above equations take the form

$$\frac{\partial P}{\partial r}=0, \tag{15}$$

$$\frac{\partial P}{\partial z}=\frac{1}{r}\frac{\partial}{\partial r}\left(r\frac{\partial w}{\partial r}\right)+\frac{1}{r}\frac{\partial}{\partial r}\left[r\left(1-d(d+b)-\frac{c}{2}(2d+3b)\right)(\lambda_1\lambda_2-\lambda_1)\left(\frac{\partial w}{\partial r}\right)^3+r(-\lambda_1^3\lambda_2)\left(1-d(d+b)-\frac{c}{2}(2d+3b)\right)^2\left(\frac{\partial w}{\partial r}\right)^5\right]-(M(r))^2(w+1). \tag{16}$$

The corresponding boundary conditions in dimensionless form are defined as

$$\begin{aligned} &w=-1 \text{ at } r=r_1,\\ &w=-1 \text{ at } r=r_2=1+\phi\sin 2\pi z. \end{aligned} \tag{17}$$

The corresponding stream function can be calculated as

$$u=-\frac{1}{r}\frac{\partial\Psi}{\partial z} \text{ and } w=\frac{1}{r}\frac{\partial\Psi}{\partial r}. \tag{18}$$

3. Solution of the Problem

3.1. HAM solution

Since (16) is a highly nonlinear equation its exact solution may be not possible. So in this section, we have found the HAM solution of (15) to (17). We choose

$$w_0=-1+\left(\frac{r^2}{4}+\frac{r_1^2-r_2^2}{4(\ln r_2-\ln r_1)}\ln r-\frac{r_1^2\ln r_2-r_2^2\ln r_1}{4(\ln r_2-\ln r_1)}\right)\frac{\partial P}{\partial z} \tag{19}$$

as the initial guess. Further, the auxiliary linear operator for the problem is taken as

$$\mathcal{L}_{wr}=\frac{1}{r}\frac{\partial}{\partial r}\left(r\frac{\partial}{\partial r}\right) \tag{20}$$

which satisfies

$$\mathcal{L}_{wr}(w_0)=0. \tag{21}$$

We can define the following zeroth-order deformation problems:

$$(1-q)\mathcal{L}_{wr}[\bar{w}(r,q)-w_0(r)]=q\hbar_w N_{wr}[\bar{w}(r,q)], \tag{22}$$

$$\begin{aligned} &\bar{w}(r,q)=-1 \text{ at } r=r_1,\\ &\bar{w}(r,q)=-1 \text{ at } r=r_2. \end{aligned} \tag{23}$$

In (22) and (23), $\hbar_w$ denote the non-zero auxiliary parameter, $q\in[0,1]$ is the embedding parameter and

$$N_{wr}[\bar{w}(r,q)]=\frac{1}{r}\frac{\partial w}{\partial r}+\frac{\partial^2 w}{\partial r^2}+\frac{1}{r}\alpha\alpha_1\left(\frac{\partial w}{\partial r}\right)^3+3\alpha\alpha_1\left(\frac{\partial w}{\partial r}\right)^2\frac{\partial^2 w}{\partial r^2}+5\alpha_2\alpha^2\left(\frac{\partial w}{\partial r}\right)^4\frac{\partial^2 w}{\partial r^2}+\frac{1}{r}\alpha_2\alpha^2\left(\frac{\partial w}{\partial r}\right)^5-\frac{\mathrm{d}P}{\mathrm{d}z}-(M(r))^2(w+1) \tag{24}$$

in which

$$\alpha=1-d(d+b)-\frac{c}{2}(2d+3b),$$
$$\alpha_1=\lambda_1\lambda_2-\lambda_1,\quad \alpha_2=-\lambda_1^3\lambda_2.$$

Obviously,

$$\hat{w}(r,0)=w_0,\quad \hat{w}(r,1)=w(r), \tag{25}$$

when q varies from 0 to 1, then $\hat{w}(r,q)$ varies from the initial guess to the solution $w(r)$. Expanding $\hat{w}(r,q)$ in Taylor series with respect to the embedding parameter q, we have

$$\hat{w}(r,q) = w_0(r) + \sum_{n=1}^{\infty} w_m(r) q^m, \tag{26}$$

$$w_m = \frac{1}{m!} \left. \frac{\partial^m \bar{w}(r,q)}{\partial q^m} \right|_{q=0}. \tag{27}$$

Differentiating the zeroth-order deformation m-times with respect to q and then dividing by $m!$ and finally setting $q = 0$, we get the following mth-order deformation problem:

$$\mathcal{L}_w[w_m(r) - \chi_m w_{m-1}(r)] = \hbar_w R_{wr}(r), \tag{28}$$

where

$$\begin{aligned} R_{wr} &= w''_{m-1} + \frac{1}{r} w'_{m-1} + \frac{1}{r} \alpha\alpha_1 \sum_{k=0}^{m-1} w'_{m-1-k} \sum_{l=0}^{k} w'_{k-l} w'_l \\ &+ 3\alpha\alpha_1 \sum_{k=0}^{m-1} w'_{m-1-k} \sum_{l=0}^{k} w'_{k-l} w''_l \\ &+ 5\alpha_2\alpha^2 \sum_{k=0}^{m-1} w'_{m-1-k} \sum_{l=0}^{k} w'_{k-l} \sum_{j=0}^{l} w'_{l-j} \sum_{i=0}^{j} w'_{j-i} w''_i \\ &+ \frac{1}{r} \alpha_2\alpha^2 \sum_{k=0}^{m-1} w'_{m-1-k} \sum_{l=0}^{k} w'_{k-l} \sum_{j=0}^{l} w'_{l-j} \sum_{i=0}^{j} w'_{j-i} w'_i \\ &- \frac{\mathrm{d}P}{\mathrm{d}z} (1-\chi_m) (M(r))^2 (w+1) \end{aligned} \tag{29}$$

with

$$\chi_m = \begin{cases} 0, & m \le 1, \\ 1, & m > 1. \end{cases} \tag{30}$$

Now two cases of MHD have been taken into account, namely

$$\text{(i) } M(r) = M \quad \text{and (ii) } M(r) = \frac{M}{r}.$$

The solution for constant MHD can be calculated with the help of Mathematica and is presented as follows:

$$\begin{aligned} w_m(r) = &\lim_{M\to\infty} \left[\sum_{m=0}^{M} a^0_{m,0} + \sum_{n=1}^{2M+1} \left(\sum_{m=n-1}^{2M} \sum_{k=1}^{2m+1-n} a^k_{m,n} r^n \ln r \right) \right] \\ &+ \lim_{M\to\infty} \left[\sum_{n=1}^{2M+1} \left(\sum_{m=n-1}^{2M} \sum_{k=0}^{2m+1-n} a^k_{m,n} r^{4n+2} \right) \right], \end{aligned} \tag{31}$$

where $a^0_{m,0}$ and $a^k_{m,n}$ are constants.

Table 1. Comparison of solutions by various methods for constant MHD case.

r	Numerical	HAM	Error
0.1	−1.00000	−1.00000	0.00000
0.2	−1.02988	−1.02972	0.00015
0.3	−1.04606	−1.04580	0.00024
0.4	−1.05338	−1.05307	0.00029
0.5	−1.05623	−1.05591	0.00030
0.6	−1.05565	−1.05534	0.00029
0.7	−1.05165	−1.05137	0.00026
0.8	−1.04538	−1.04514	0.00022
0.9	−1.03679	−1.03660	0.00018
1.0	−1.02468	−1.02457	0.00010
1.1	−1.01159	−1.01153	0.00005
1.18	−1.00000	−1.00000	0.00000

Table 2. Comparison of solutions by various methods for variable MHD case.

r	Numerical	HAM	Error
0.1	−1.00000	−1.00000	0.00000
0.2	−1.03235	−1.03171	0.00062
0.3	−1.05212	−1.05151	0.00058
0.4	−1.06290	−1.06234	0.00052
0.5	−1.06873	−1.06821	0.00048
0.6	−1.07023	−1.06974	0.00045
0.7	−1.06723	−1.06676	0.00044
0.8	−1.06053	−1.06008	0.00042
0.9	−1.05016	−1.04974	0.00040
1.0	−1.03440	−1.03406	0.00032
1.1	−1.01643	−1.01624	0.00018
1.18	−1.00000	−1.00000	0.00000

3.2. Numerical Solution

The present problem consisting of (16) to (18) is also solved numerically by employing the shooting method. The numerical results are compared with the HAM results, and we have found a very good agreement between both results (see Table 1).

The solution for variable MHD case can be calculated with the help of Mathematica and is presented as follows:

$$\begin{aligned} w_m(r) = &\lim_{M\to\infty} \left[\sum_{m=0}^{M} l^0_{m,0} + \sum_{n=1}^{2M+1} \left(\sum_{m=n-1}^{2M} \sum_{k=1}^{2m+1-n} l^k_{m,n} r^n \ln r \right) \right] \\ &+ \lim_{M\to\infty} \left[\sum_{n=1}^{2M+1} \left(\sum_{m=n-1}^{2M} \sum_{k=0}^{2m+1-n} l^k_{m,n} r^{4n+2} \right) \right], \end{aligned} \tag{32}$$

where $l^0_{m,0}$ and $l^k_{m,n}$ are constants.

4. Numerical Results and Discussion

To observe the convergence region and the variations in the velocity profile caused by the relaxation

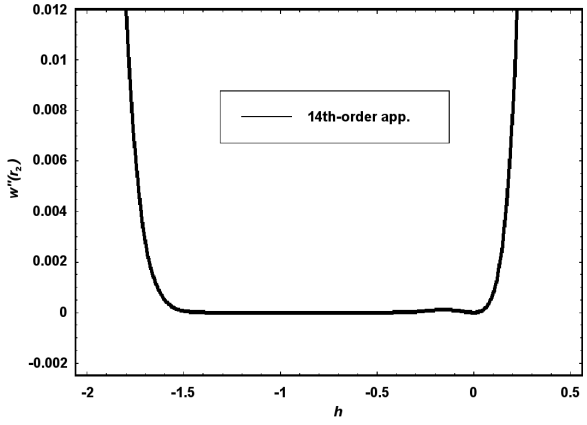

Fig. 2. h-curve for the velocity profile for $\varepsilon = 0.1$, $\lambda_1 = 0.5$, $\lambda_2 = 0.5$, $z = 0.1$, $\mathrm{d}P/\mathrm{d}z = 0.35$, $\phi = 0.3$, $d = 0.1$, $b = 0.4$, $c = 0.4$.

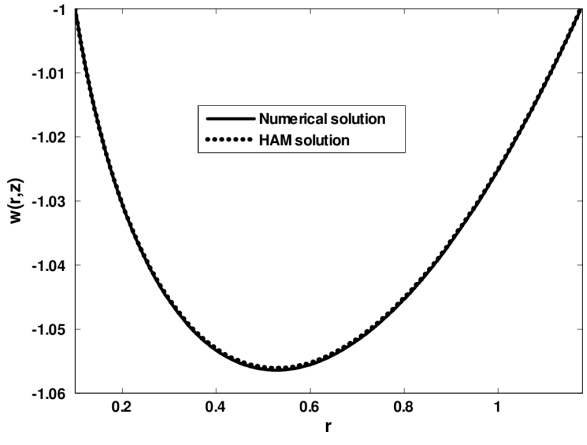

Fig. 3. Comparison of the velocity field for $\varepsilon = 0.1$, $\lambda_1 = 0.5$, $\lambda_2 = 0.5$, $z = 0.1$, $\mathrm{d}P/\mathrm{d}z = 0.35$, $\phi = 0.3$, $h = -1$, $d = 0.1$, $b = 0.4$, $c = 0.4$, $M = 0.6$.

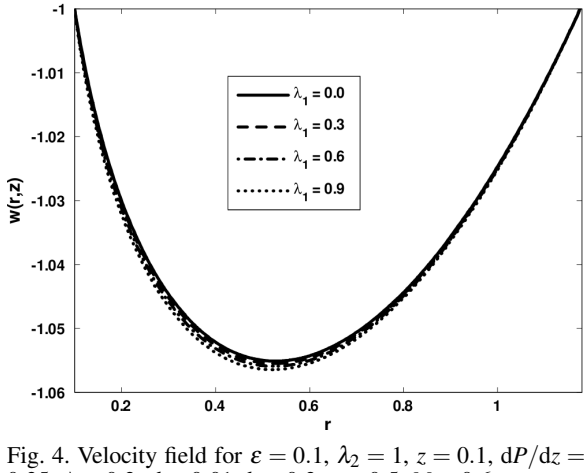

Fig. 4. Velocity field for $\varepsilon = 0.1$, $\lambda_2 = 1$, $z = 0.1$, $\mathrm{d}P/\mathrm{d}z = 0.35$, $\phi = 0.3$, $d = 0.01$, $b = 0.3$, $c = 0.5$, $M = 0.6$.

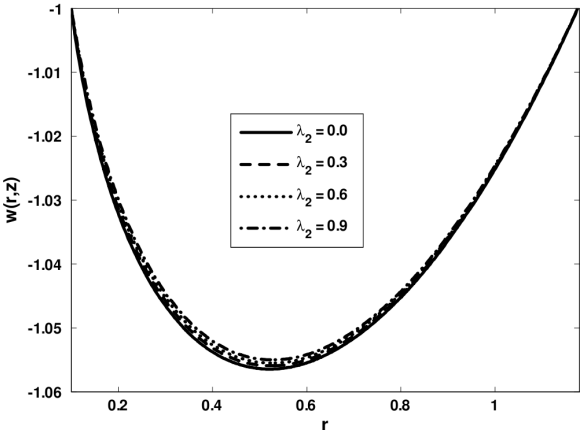

Fig. 5. Velocity field for $\varepsilon = 0.1$, $\lambda_1 = 1$, $z = 0.1$, $\mathrm{d}P/\mathrm{d}z = 0.35$, $\phi = 0.3$, $d = 0.01$, $b = 0.3$, $c = 0.5$, $M = 0.6$.

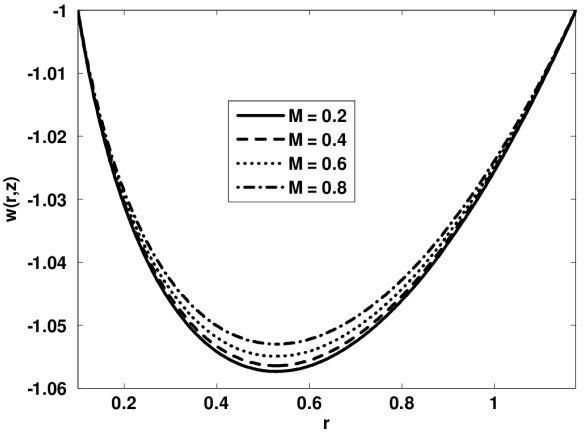

Fig. 6. Velocity field for $\varepsilon = 0.1$, $\lambda_1 = 0.5$, $z = 0.1$, $\mathrm{d}P/\mathrm{d}z = 0.35$, $\phi = 0.3$, $d = 0.01$, $b = 0.3$, $c = 0.5$, $\lambda_2 = 0.5$.

time λ_1, retardation time λ_2, and Hartmann number M, we have plotted Figures 2 to 11. Figures 2 to 6 show the physical behaviour of different parameters for constant MHD case. Figure 2 shows the convergence region for the velocity profile. Figure 3 represents the comparison of the velocity profile for both HAM and numerical results. The graph shows a very good agreement between both results. It is seen from Figures 4 to 6 that with the increase in the values M and λ_2, the velocity profile increases while an increase in λ_1 causes decrease in the velocity profile. Figure 7a, b illustrate the streamline graphs for different values of Hartmann number M. It is observed that when we increase M the size of trapped bolus increases. Figure 7c, d show the streamlines for λ_1 (Jeffrey parameter). It is analyzed that with increasing λ_1 the number of trapped bolus

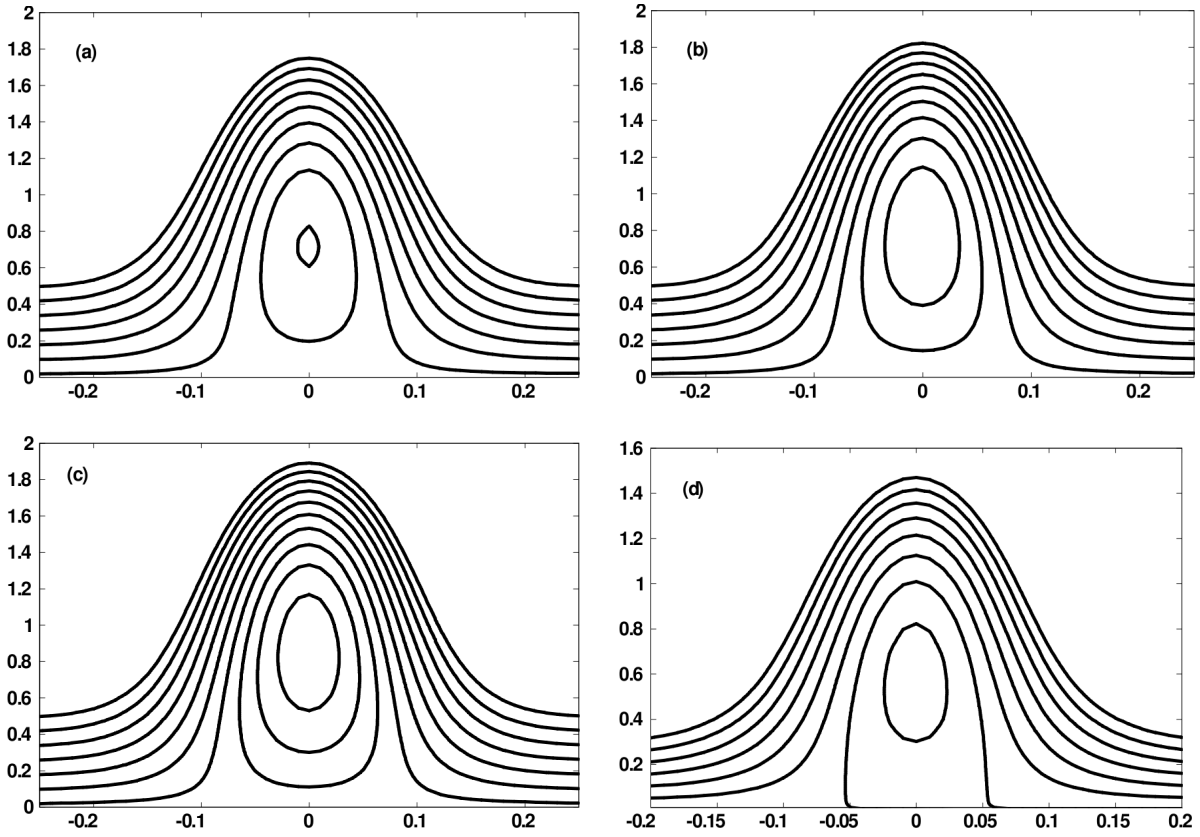

Fig. 7. Streamlines for different values of $M = 1$ (a) and $M = 2$ (b). The other parameters are $\varepsilon = 0.1$, $\lambda_2 = 1$, $z = 0.1$, $\mathrm{d}P/\mathrm{d}z = 0.35$, $\phi = 0.3$, $d = 0.01$, $b = 0.3$, $c = 0.5$, $\lambda_1 = 0.2$. Streamlines for different values of $\lambda_1 = 0.1$ (c) and $\lambda_1 = 0.2$ (d). The other parameters are $\varepsilon = 0.1$, $\lambda_2 = 1$, $z = 0.1$, $\mathrm{d}P/\mathrm{d}z = 0.35$, $\phi = 0.3$, $d = 0.01$, $b = 0.3$, $c = 0.5$, $M = 2$.

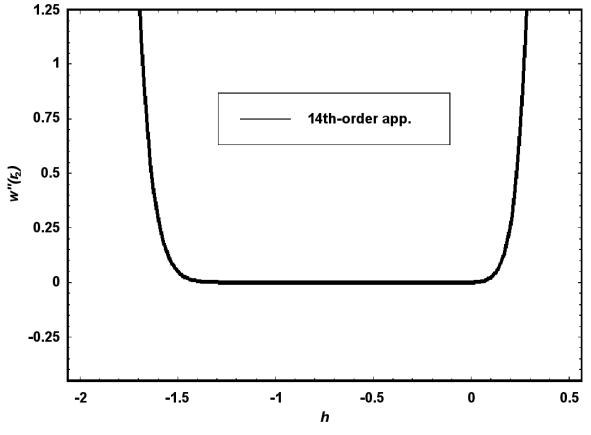

Fig. 8. h-curve for the velocity profile for $\varepsilon = 0.1$, $\lambda_1 = 0.5$, $\lambda_2 = 2$, $z = 0.1$, $\mathrm{d}P/\mathrm{d}z = 0.56$, $\phi = 0.3$, $d = 0.1$, $b = 0.3$, $c = 0.4$.

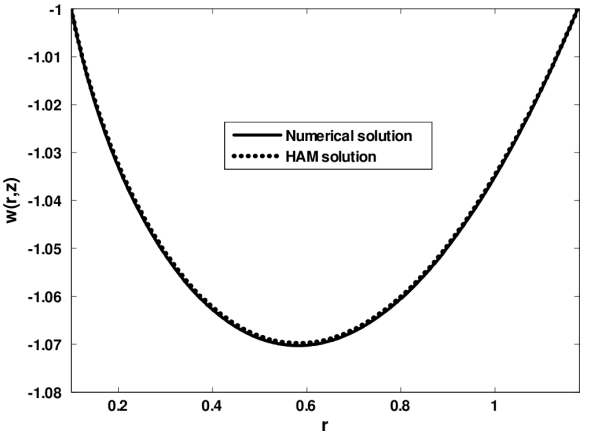

Fig. 9. Comparison of the velocity profile for $\varepsilon = 0.1$, $\lambda_1 = 0.5$, $\lambda_2 = 2$, $z = 0.1$, $\mathrm{d}P/\mathrm{d}z = 0.56$, $\phi = 0.3$, $d = 0.1$, $b = 0.3$, $c = 0.4$, $h = -1$.

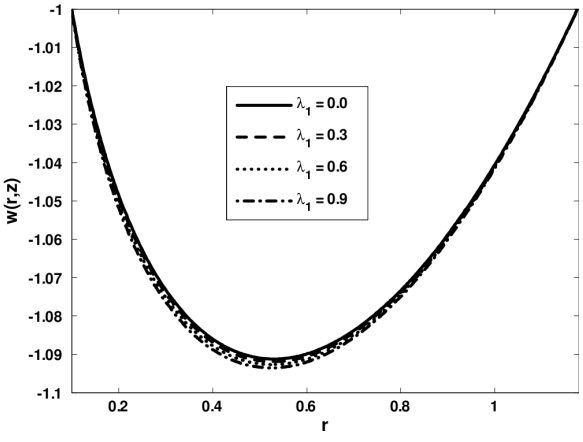

Fig. 10. Velocity field for $\varepsilon = 0.1$, $\lambda_2 = 0.5$, $z = 0.1$, $\mathrm{d}P/\mathrm{d}z = 0.56$, $\phi = 0.3$, $d = 0.01$, $b = 0.3$, $c = 0.5$, $M = 0.05$.

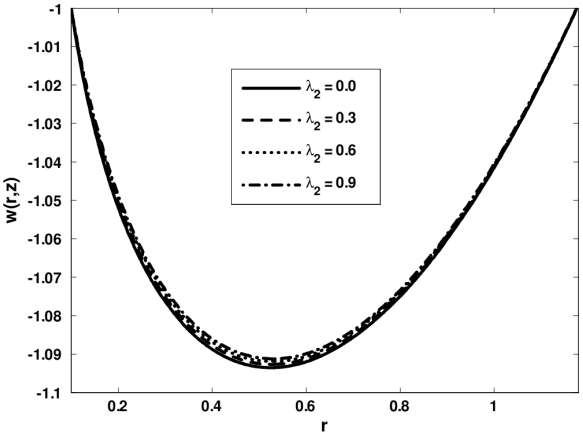

Fig. 11. Velocity field for $\varepsilon = 0.1$, $\lambda_1 = 0.5$, $z = 0.1$, $\mathrm{d}P/\mathrm{d}z = 0.56$, $\phi = 0.3$, $d = 0.01$, $b = 0.3$, $c = 0.5$, $M = 0.05$.

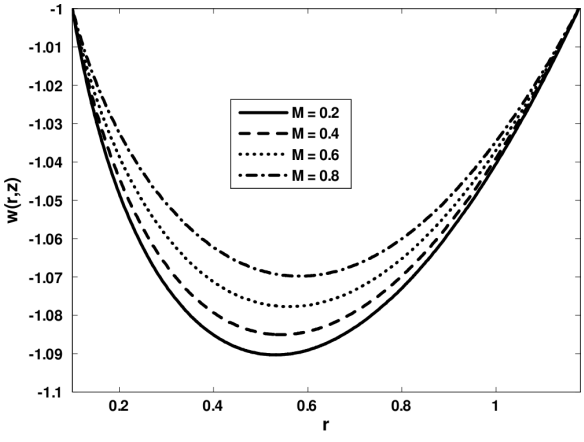

Fig. 12. Velocity field for $\varepsilon = 0.1$, $\lambda_2 = 0.5$, $z = 0.1$, $\mathrm{d}P/\mathrm{d}z = 0.56$, $\phi = 0.3$, $d = 0.01$, $b = 0.3$, $c = 0.5$, $\lambda_2 = 0.5$.

decreases but their size increases. The physical behaviour of different parameters for variable MHD case can be seen from Figures 8 to 12. Figure 8 indicates the convergence region for the velocity profile. Figure 9 shows the comparison of the velocity profile for both HAM and numerical results. It is depicted from Figures 10 to 12 that an increase in the values M and λ_2 causes an increase in the velocity profile while with the increase in λ_1 velocity profile decreases. Figures 13 plotted to show the effects of Hartmann number M and Jeffrey parameter λ_1 on the streamlines. It is seen that the number of trapped bolus increases and their size decreases with an increase in M and the size of trapped bolus increases with the increase in λ_1.

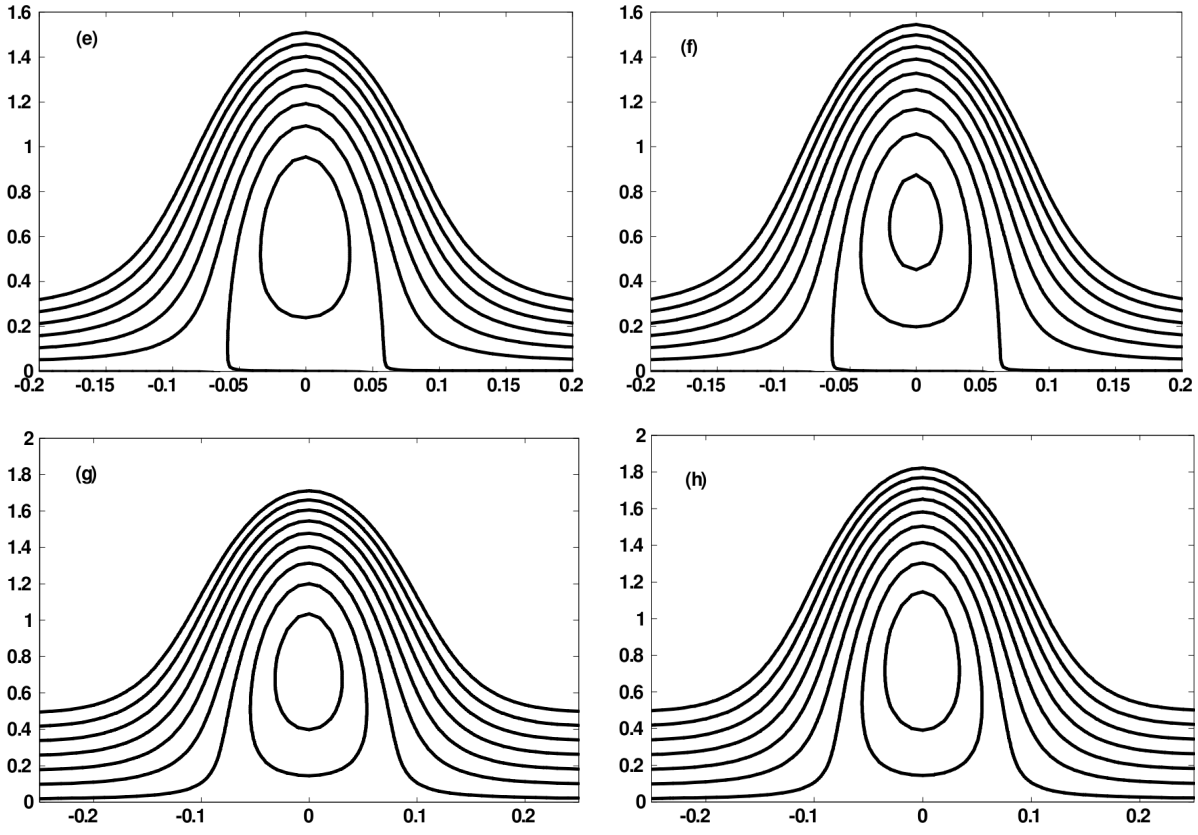

Fig. 13. Streamlines for different values of $M = 1$ (e) and $M = 2$ (f). The other parameters are $\varepsilon = 0.1$, $\lambda_2 = 1$, $z = 0.1$, $\mathrm{d}P/\mathrm{d}z = 0.35$, $\phi = 0.3$, $d = 0.01$, $b = 0.3$, $c = 0.5$, $\lambda_1 = 0.2$. Streamlines for different values of $\lambda_1 = 0.1$ (g) and $\lambda_1 = 0.2$ (h). The other parameters are $\varepsilon = 0.1$, $\lambda_2 = 1$, $z = 0.1$, $\mathrm{d}P/\mathrm{d}z = 0.35$, $\phi = 0.3$, $d = 0.01$, $b = 0.3$, $c = 0.5$, $M = 2$.

[1] S. Srinivas and R. Gayathri, Appl. Math. Comput. **215**, 185 (2009).
[2] S. Nadeem and N. S. Akbar, Z. Naturforsch. **64a**, 713 (2009).
[3] S. Nadeem and N. S. Akbar, Int. J. Numer. Methods Fluids 2009, DOI:10.1002/fld.2253.
[4] K. Vajravelu, S. Sreenadh, and V. Ramesh Babu, Appl. Math. Comput. **169**, 726 (2005).
[5] K. Vajravelu, S. Sreenadh, and V. Ramesh Babu, Int. J. Nonlinear Mech. **40**, 83 (2005).
[6] E. F. Elshehawey, N. T. Eladabe, E. M. Elghazy, and A. Ebaid, Appl. Math. Comput. **182**, 140 (2006).
[7] M. Ealshahed and M. H. Haroun, Math. Probl. Eng. **6**, 663 (2005).
[8] M. H. Haroun, Comput. Mat. Sci. **39**, 324 (2007).
[9] A. El. Hakeem, A. EI Naby, A. E. M. El Misery, and I. I. El Shamy, J. Phys. A. **368**, 535 (2003).
[10] S. Srinivas, R. Gayathri and M. Kothandapani, Comput. Phys. Commun. **180**, 2115 (2009).
[11] A. Barletta, S. Lazzari, E. Magyari, and I. Pop, Int. J. Heat Mass Transfer **51**, 5777 (2008).
[12] T. Hayat, F. M. Mahomed, and S. Asghar, Nonlinear Dyn. **40**, 375 (2005).
[13] S. Srinivas and M. Kothandapani, Math. Comput. **213**, 197 (2009).
[14] S. Nadeem and N. S. Akbar, Commun. Nonlinear Sci. Numer. Simul. **14**, 3844 (2009).
[15] S. Nadeem, N. S. Akbar, and M. Hameed, Int. J. Numer. Methods Fluids 2009, DOI:10.1002/fld.2134.
[16] S. Srinivas and M. Kothandapani, Appl. Math. Comput. **213**, 197 (2009).
[17] S. N. Aristov, O. I. Skul'skii, J. Appl. Mech. Tech. Phys. **43**, 817 (2002).